Doping- and Momentum-Dependent Superconducting Gap of Bilayer Cuprate $Bi_2Sr_2CaCu_2O_{8+\delta}$ Revealed Using Low-energy ARPES

Hiroaki ANZAI[1,a,*], Masashi ARITA[2], Hirofumi NAMATAME[2],
Masaki TANIGUCHI[2], Motoyuki ISHIKADO[3], Kazuhiro FUJITA[4],
Shigeyuki ISHIDA[5], Shinichi UCHIDA[6], Akihiro INO[2]

[1]Graduate School of Engineering, Osaka Prefecture University, Sakai 599-8531, Japan

[2]Hiroshima Synchrotron Radiation Center, Hiroshima University, Higashi-Hiroshima 739-0046, Japan

[3]Comprehensive Research Organization for Science and Society, Tokai, Ibaraki 319-1106, Japan

[4]Department of Physics, Cornell University, Ithaca, New York 14853, USA

[5]Advanced Industrial Science and Technology, Tsukuba, Ibaraki 305-8568, Japan

[6]Department of Physics, University of Tokyo, Tokyo 113-0033, Japan

[a]anzai@ms.osakafu-u.ac.jp

*Corresponding author

Keywords: High-T_c Superconductivity, Angle-resolved Photoemission Spectroscopy.

Abstract. We report a systematic study of angle-resolved photoemission spectroscopy on $Bi_2Sr_2CaCu_2O_{8+\delta}$ by using low-energy synchrotron radiation. Our focus is on delineating the doping- and momentum-dependent superconducting gap of the bilayer split bands, which are associated with the intracell hybridization of electrons between the two CuO_2 planes. From highly detailed information of gap profile along Fermi surfaces of bonding and antibonding bands, we revealed that a transition temperature T_c is proportional to a nodal-gap energy Δ_N. This result is quantitatively consistent with our findings that the nodal-gap component $2\Delta_N$ is relevant to the antinodal-gap energy Δ^* through a reduction factor of square-root superfluid density ρ_s, as formulated by $8.5k_BT_c = 2\Delta_N \propto \Delta^*\sqrt{\rho_s}$. This empirical formula makes an essential contribution to the mechanisms for the unconventional superconductivity.

Introduction

Over the past three decades, identification of a key parameter responsible to the high-T_c superconductivity has been a central issue in the research of cuprates. In the conventional superconductors, a superconducting critical temperature T_c is proportional to an energy gap, which opens in the electronic excitation spectrum and stands for both the electron-pairing energy and the superconducting order parameter[1]. Hence, the energy gap is one of the leading parameters for the high-T_c superconductivity. Two contrasting behaviors have been identified among the gaps determined with various probes in the superconducting state[2, 3, 4]. One is an amplitude of d-wave-like gap Δ^*, which increases as T_c decreases in the underdoped region. This energy remains as a pseudogap above T_c and typically seen in the electronic excitation spectra around the antinode[5]. The other is a near-nodal gap, which decreases like T_c with underdoping[6, 7]. Recently, we have suggested that the nodal-gap component Δ_N at the nodal limit of the gap slope closely follows $8.5k_BT_c$ and concomitantly relates to the antinodal-gap energy Δ^* through a reduction factor of square-root superfluid density ρ_s[8]. This scaling relation is different from phase competition behavior between the pseudogap and superconductivity, where the nodal-gaps are independent of the doping at $0.08 < p < 0.19$[9]. To establish the appropriate theoretical framework for the high-T_c superconductivity, it is important to explore the relation among the two gaps and T_c at various dopings and in bilayer split bands of $Bi_2Sr_2CaCu_2O_{8+\delta}$ (Bi2212).

Angle-resolved photoemission spectroscopy (ARPES) is a direct probe to measure the electronic excitation spectrum as a function of momentum. In the previous ARPES studies, extracting the nodal gap, Δ_0, has been inferred from the slope of gap profile under a standard d-wave form $\Delta(\theta) = \Delta_0 \sin 2\theta$[6, 9]. The problem is that it is difficult to determine the nodal gap from only a few momentum-sampling steps in the Brillouin zone. Such insufficient momentum resolution leads to an overestimation of Δ_0. Moreover, in the case of Bi2212, the energy band splits into the bonding (BB) and antibonding band (AB) due to the interaction between two proximate CuO_2 planes. Their quasiparticle properties have been neglected[6, 9]. To address these problems, we utilized low-energy synchrotron radiation in the ARPES measurements[10,11,12]. Taking advantages of high energy- and momentum-resolution, and photon-energy tunability, we determined the details of the doping and momentum dependence of the gap energies of Bi2212.

Experiment

High-quality single crystals of Bi2212 were grown by the traveling-solvent floating-zone method. Hole concentration p was deduced from T_c of the sample using an empirical relation of $T_c / T_c^{max} = 1 - 82.6(p - 0.16)^2$, where T_c^{max} is 91 K. We labeled the samples with the value of T_c and the doping range for underdoped (UD), optimally-doped (OP) or overdoped (OD). For example, an underdoped sample with $T_c = 66$ K is denoted as UD66. The ARPES experiments were performed at BL-9A of Hiroshima Synchrotron Radiation Center. The total energy resolution was set to 5 meV. All the samples were cleaved *in situ* under ultra-high vacuum better than 5×10^{-11} Torr and measured at $T = 10$ K.

Results and Discussion

Figure 1 shows low-energy ARPES spectra of Bi2212 at three typical doping levels. Using $h\nu = 8.5$ eV photon energy, the bilayer bands of OD80 and OP91 were clearly observed from the node (#1) to intermediate region (#6). Despite a difficulty in controlling surface quality, a nodal bilayer splitting, $k^{BS} = 0.008$ Å^{-1}, was resolved for UD66, as shown in #1 of Fig.1(b). We confirmed carefully the coexistence of the two bands from the second derivative analysis of the ARPES spectra in the intermediate region (#2-#6) for other underdoped samples. The superconducting gap opens gradually away from the node, indicating the form of d-wave-like gap. We rigorously determined Fermi surfaces from the minimum-gap loci and extracted the superconducting gap along the Fermi surfaces of the BB and AB.
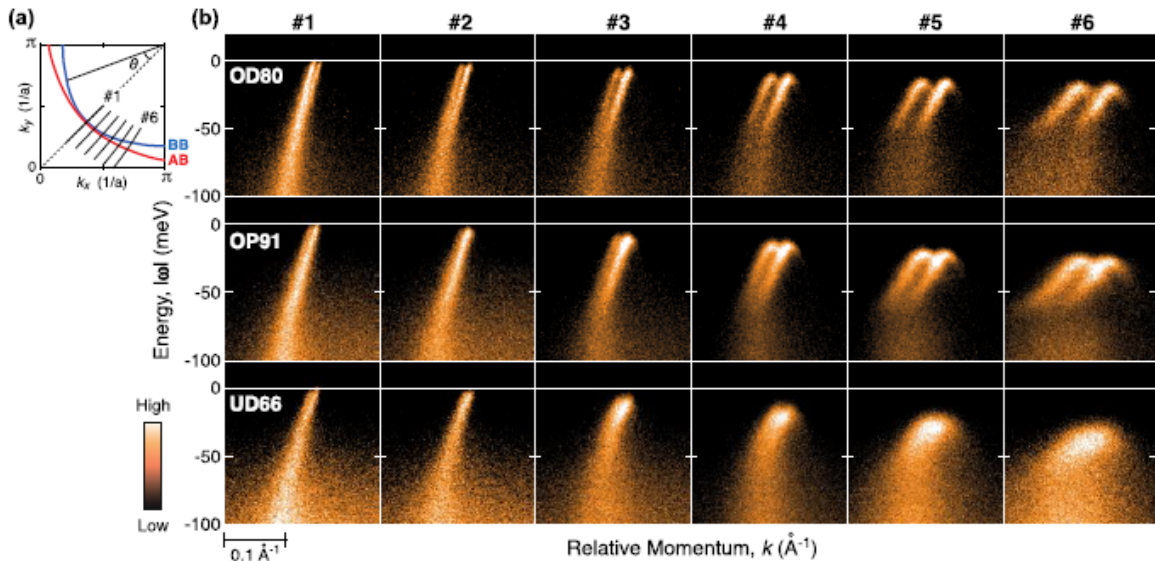

Fig.1 Low-energy Synchrotron-radiation ARPES Data of Bilayer Cuprate Bi2212

The data were collected at $T = 10$K with $h\nu = 8.5$eV. (**a**) Schematic Fermi surfaces of the bonding band (BB) and antibonding band (AB). Off-node angle is defined about (π, π) point. (**b**) ARPES spectra along typical momentum cuts as indicated white corves in (**a**).

Figures 2(a)-(f) show the gap profiles of Bi2212 as a function of off-node angle θ, where θ is referenced to the nodal direction (Fig. 1(a)). Sharp quasiparticle peaks were observed in the energy distribution curves (EDCs) at the minimum-gap loci of the BB and AB. We found that the peak positions, corresponding to the gap magnitudes, $\Delta(\theta)$, are comparable between the BB and AB within error bars, as shown in Figs. 2(g)-(i). This result indicates that the pairing strength is nealy identical for the bilayer bands. In Figs. 2(a)-2(f), we plot the gap profiles as a function of θ. Whereas the profile of OP91 and OD80 is almost a straight line, the profile of UD66 exhibits a curve. It should be noted that slope of the gap profile of UD66 decreases asymptotically toward the node. As shown in Figs. 2(g)-(i), spectral features of the peak width and intensity, smoothly evolve from the node to antinode. This continuous evolution of the spectra with momenta has also been reported by Vishik *et al.*[13]. To further investigate the doping- and momentum-dependent gap profile, we extracted a pure nodal gap component, Δ_N, by using a high-harmonic fitting function of $\Delta(\theta) = \Delta_N \sin 2\theta + (\Delta^* - \Delta_N)(3\sin 2\theta - \sin 6\theta)/4$, where the first term is solely responsible for the nodal-gap slope, and the second term models the gap deviation without adjustable angle parameter[14, 15]. The nodal and antinodal gap energies are defined as $\Delta_N = 0.5(d\Delta/d\theta)\big|_{\theta=0^\circ}$ and $\Delta^* = \Delta(\theta)\big|_{\theta=45^\circ}$, respectively, so that $\Delta_N / \Delta^* = 1$ is satisfied for the ideal *d*-wave gap as depicted in Fig.2(b). This function well captures the curved gap profiles, as indicated by a black curve in Figs.2(a)-(f). We determined the nodal tangents $\Delta_N\sin 2$ (blue lines) for all the doping levels. One can find that the nodal limit of the gap slope increases from OD80 to OP91 and then decreases at UD66, whereas the antinodal features are increases with underdoping.
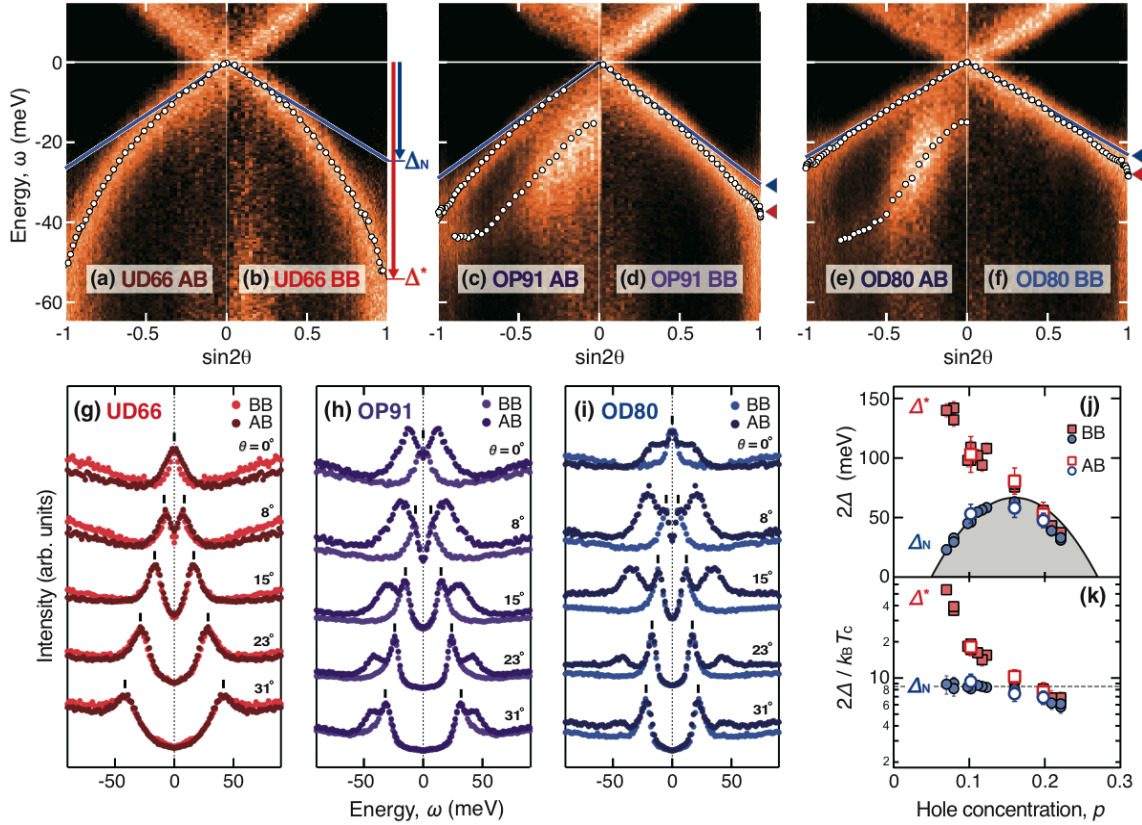

Fig.2 Superconducting Gaps Observed for the Bonding Band and the Antibonding Band

(**a**)-(**f**) Energy-versus-sin2θ plots of gap profiles for UD66, OP91, and OD80. The images are symmetrized with respect to $\omega = 0$. Left and right images are data for AB and BB, respectively. Open

circle, black curve, and blue line denote gap energy, high-harmonic fit, and nodal tangent, respectively. (**g**)-(**i**) EDCs taken from data in (**a**)-(**f**). (**j**) Doping dependence of the nodal gap Δ_N (circles) and antinodal gap Δ^* (squares). Black curve indicates the empirical relation of the hole concentration. (**k**) Same as (**j**), but scaled by T_c. The original data for BB in (**b**), (**d**), (**f**), (**j**) and (**k**) have been reported in Ref. 8.

Two gap parameters, Δ_N and Δ^*, are plotted as a function of hole concentration in Fig. 2(j) together with the data for the BB reported in Ref. 8. As hole concentration p decreases from the overdoped limit, both the nodal and antinodal gaps increase with keeping a constant proportion, $\Delta_N = 0.87\Delta^*$. This is the canonical behavior expected when the coupling is getting stronger. With further decreasing p, the nodal gap $2\Delta_N$ follows the decrease in T_c in contrast to the monotonic increase in the antinodal gap Δ^*. As shown in Fig. 2(k), the gap-to-T_c ratio is estimated to be $2\Delta_N/k_BT_c = 8.5$ from the optimum to underdoped levels. This value is about twice the mean-field prediction 4.3 for d-wave weak-coupling superconductors and is nearly independent of the bilayer bands. It is reasonable that T_c is determined primarily by Δ_N rather than Δ^*, because thermal quasiparticle excitations concentrate in the vicinity of the node and hardly occur around the antinode in particular for strong-coupling case, $2\Delta^*/k_BT_c \gg 4.3$. The association between the nodal excitations and T_c has also been suggested in various experiments[6,16,17,18].

The data reported here is quantitatively consistent with the previous our findings [8]. The square of nodal-to-antinodal gap ratio, $(\Delta_N / \Delta^*)^2$ exhibits a clear resemblance to the doping dependence of the superfluid density ρ_s, which increases linearly in p with an onset at $p \sim 0.07$ and saturates at $p \sim 0.19$[19, 20]. As a result, we obtained another proportional relation, $\Delta_N/\Delta^* \propto \sqrt{\rho_s}$. The form of $\Delta_{SC}/\Delta = \sqrt{\rho_s/\rho_s^{BCS}}$ has been theoretically deduced for the superfluid reduction due to incoherent pair excitations inherent in the strong-coupling superconductors, where the degeneracy between the order parameter Δ_{SC} and the pair-formation energy is split. Taking into account the lifetime effect, the former is manifested in the energy of the near-nodal spectral peak as Δ_N, and the latter dominates the antinodal peak energy Δ^*[21, 22]. The superfluid density in the weak-coupling BCS model, ρ_s^{BCS}, should be approximated by a constant, because the Fermi velocity and Fermi-surface perimeter in the normal state are hardly dependent on the hole concentration[23]. Therefore, our empirical relation, $\Delta_N/\Delta^* \propto \sqrt{\rho_s}$, with $\rho_s^{BCS} \cong 31$ μm^{-2}, is explained the strong-coupling scenario well, and it is consistent with the fact of the high gap-to-T_c ratios in Fig.2(k). Combining the two relations, we obtain $8.5k_BT_c = 2\Delta_N \propto \Delta^*\sqrt{\rho_s}$. This formulation associates T_c with the superfluid density ρ_s, as well as with the pair-formation energy, $\Delta \simeq \Delta^*$. Regardless of interpretation, this simple relation among the fundamental parameters makes a advance in understanding the high-T_c superconductivity, and will stimulate broad activities with its simplicity and universality.

Summary

In conclusion, we have studed the doping- and momentum-dependent superconducting gap of Bi2212 using low-energy ARPES. A simple proportional relation between the nodal gap and critical temperature is revealed and described as $2\Delta_N = 8.5k_BT_c$, which is nearly independent of the bilayer bands. On the basis of a comparison with the superfluid density, we suggest finally simple formulae, $8.5k_BT_c = 2\Delta_N \propto \Delta^*\sqrt{\rho_s}$. This equation will provide a new gap-based perspective on the principle governing T_c in strong-coupling superconductors.

Acknowledgement

References

[1]   J. R. Schrieffer, Theory of Superconductivity (Addison-Wesley, New York, 1964).

[2]   S. Hüfner, M. A. Hossain, A. Damascelli and G. A. Sawatzky, Rep. Prog. Phys. 71, 062501 (2008).

[3]   M. Le Tacon et al., Nature Phys. 2, 537–543 (2006).

[4]   J. W. Alldredge et al., Nature Phys. 4, 319–326 (2008).

[5]   A. G. Loeser et al., Science 273, 325–329 (1996).

[6]   W. S. Lee et al., Nature 450, 81–84 (2007).

[7]   A. Pushp et al., Science 324, 1689–1693 (2009).

[8]   H. Anzai et al., Nature Commun. 4, 1815 (2013).

[9]   I. M. Vishik et al., Proc. Natl Acad. Sci. USA 109, 18332–18337 (2012).

[10]   T. Yamasaki et al., Phys. Rev. B 75, 140513 (2007).

[11]   H. Anzai et al., Phys. Rev. Lett. 105, 227002 (2010).

[12]   A. Ino et al., Nanoscale Research Letters 8, 515 (2013).

[13]   I. M. Vishik et al., Nature Phys. 5, 718–721 (2009).

[14]   J. Mesot, et al., Phys. Rev. Lett. 83, 840–843 (1999).

[15]   Y. Kohsaka et al., Nature 454, 1072–1078 (2008).

[16]   M. Le Tacon et al., Nature Phys. 2, 537–543 (2006).

[17]   J. W. Alldredge et al., Nature Phys. 4, 319–326 (2008).

[18]   A. Pushp et al., Science 324, 1689–1693 (2009).

[19]   J. L. Tallon, J. W. Loram, J. R. Cooper, C. Panagopoulos and C. Bernhard, Phys. Rev. B 68, 180501R (2003).

[20]   W. Anukool, S. Barakat, C. Panagopoulos and J. R. Cooper, Phys. Rev. B 80, 024516 (2009).

[21]   Q. Chen, I. Kosztin, J. Boldizsár and K. Levin, Phys. Rev. Lett. 81, 4708–4711 (1998).

[22]   C.-C. Chien, Y. He, Q. Chen and K. Levin, Phys. Rev. B 79, 214527 (2009).

[23]   T. K. Kim et al., Phys. Rev. Lett. 91, 167002 (2003).